# Monitoring of shear strain in shallow sections of slopes to detect increased risk of slope failure

## La détection des stress dus aux cisaillements dans les parties peu profondes des plans inclinés pour déterminer les risques d'effondrements

S. Tamate and K. Itoh
*National Institute of Occupational Safety and Health, Japan*

ABSTRACT
Slope failures frequently cause labour accidents in construction sites, and even a small collapse can cause serious injury to workers. The Short Pipe Strain transducer (*SPS*) was developed to measure shear strain increments in the shallow section of slopes, and its applicability was examined through centrifuge model tests and prototype model tests. Prior to slope failure, obvious increases in the response of strain ($r_s$) were measured during slope cutting tests. In loam ground, creep strain curves were observed. A couple of minutes can be provided by monitoring the second or third creep. Accordingly, it was confirmed that the *SPS* not only measures slope movement but also senses an increase in the risk of slope failure. Slope inspections must be conducted to ensure safety during work, and the *SPS* is effective for subsidiary warning systems that save workers' lives.

RÉSUMÉ
Les effondrements causés par une inclinaison des surfaces, dans les ouvrages de construction, sont une cause fréquente d'accidents de travail. Il est notoire qu'un effondrement peut avoir de désastreuses conséquences pour un ouvrier; celui-ci peut se blesser gravement. Le détecteur de tension, appelé Short Pipe Strain transducer (*SPS*), (le convecteur de tension de tuyaux courts) a été développé pour mesurer les variations dues aux cisaillements dans les parties peu profondes des inclinaisons. L'efficacité de l'instrument a par la suite été mesurée par des essais centrifuges et sur des prototypes. Des augmentations notables dans les réponses de tensions ($r_s$) ont été mesurées tenant compte des coupures faites sur les plans inclinés; ceci avant que les bris soient survenus. Sur les sols lâches, des courbes produites pas les tensions dues aux glissements ont été notées. Deux minutes pourraient être fournies en surveillant le 2e ou 3e glissement. Par conséquent il s'est avéré qu'en plus de le mouvement des inclinaisons, le SPS détecte le risque qu'une inclinaison se brise. Il est nécessaire d'inspecter les inclinaisons des surfaces si l'on veut éviter les accidents pendant des travaux; le SPS est un système d'avertissement d'accompagnement qui a pour effet de sauver la vie des ouvriers.

Keywords: slope failure, labor accident, monitoring, shear strain in shallow section, prototype model test, centrifuge model test

## 1 INTRODUCTION

Labour accidents due to slope failure frequently occur at construction work sites, and even a small collapse can cause serious injury to workers. Such casualties reach around 50 per year in Japan. One can assume that the same problem exists throughout the world. Many failures occur during the slope cutting process, and the risk of slope failure usually increases as the cutting progresses.

Slope failure must be avoided to ensure safety: temporary retaining walls are needed to support slopes during work, and drills practicing rapid escape are important to save workers' lives. Warnings must be given prior to slope failure, and for this reason slope monitoring is needed to detect any increased risk of failure.

This paper first summarizes hazards existing at slope works and examines occupational accidents there. The paper then introduces a developed simple monitoring device, the Short Pipe Strain transducer (*SPS*), which can be used to measure shear strain increments in shallow sections of slopes. Finally, applicability of the *SPS* is discussed, based on the results of prototype model tests and centrifuge model tests.

## 2 LABOR ACCIDENTS CAUSED BY SLOPE FAILURE

Excavations and cuttings are frequently done during many aspects of slope works. A cutting at the toe of a slope is usually made as part of the process of building retaining walls. However, even though its duration is short term, a cutting can cause instability in the slope. Itoh et al. (2005) reported that 164 accidents occurred due to unstable slopes between 1989 and 2001. The volume of collapsed soil blocks in about 60% of those accidents was less than 50m$^3$.

Figure 1 shows a labour accident caused by slope failure at a construction site. Small gravity walls were constructed to support an unstable slope. However, a small failure occurred in the upper right side of the slope. Cuttings at the toe, without temporary supports, caused slope instability. A worker in the lower part of the works was crushed by collapsing soil that slid down rapidly during the failure. In many such cases, not enough time is given for people working nearby to escape. A warning prior to such a slope failure is important to protect workers, in addition to the installation of temporary supports at unstable slopes.

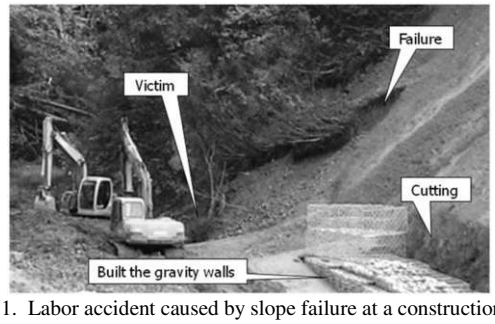

Figure 1. Labor accident caused by slope failure at a construction site



*doi:10.3233/978-1-60750-031-5-2143*

## 3 DEVELOPED MONITORING DEVICE

### 3.1 *Shape and structure of the developed SPS*

The *SPS* was developed to measure shear strain at shallow sections of slopes, using its bending deformation ability (Tamate et al. (2007)). The *SPS* is compact: 1m in length, 15mm in diameter, and 4.9N in weight, as shown in Figure 2. A screw point 100mm in length is attached to the lower end, enabling the device to penetrate into the ground without pre-boring. A connector 100mm in length attached to the upper end is composed of a chuck and a socket. The socket covers 12 poles of terminals.

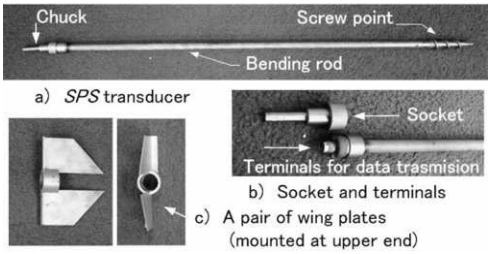


Figure 2. *SPS* components

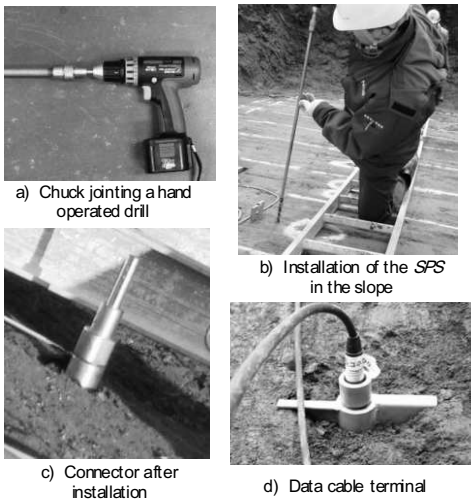


Figure 3. *SPS* installation

### 3.2 *Strain perception using bending deformation*

A bending rod 800mm in length is positioned between the screw point and the connector. The bending rod has a double pipe structure, consisting of an inner and outer pipe. A couple of strain gauges are attached to both the front and back of the inner pipe, to register increases in strain output that are determined by increased bending deformation. The outer pipe protects the gauges after installation. The hollow structure also contributes by lightening the unit body. An epoxy adhesive liquid fills the space between the inner and outer pipes to decrease transmission loss during bending deformations.

### 3.3 *SPS installation*

Easy installation is achieved with the *SPS* because the screw point enables penetration into the ground without pre-boring. The installation process is shown in Figure 3, and is explained as follows.

1) *SPS* connection: Either a hand drill or a wrench connects to the *SPS* chuck.

2) Drilling: The *SPS* is installed at a 90 degree angle to the slope surface. Penetration took less than 1 minute when hand drills were used in the prototype model tests.

3) Plate connection: The chuck is removed after installation of the *SPS*, then the wing plate is connected at the upper end to improve response to slope movement.

4) Cable connection: A cable for data transmission connects to the terminals at the upper end of the *SPS*. Strain output data is collected by data acquisition devices.

A complete installation can be done by one person in a couple of minutes.

Table 1. Codes and conditions in prototype model tests

| Codes | Cs1 | Cs2 | Cs3 |
|---|---|---|---|
| Soil material | Kanto loam | Kanto loam | Narita sand |
| Number of rolling compactions | 0 (Softer) | 5 (Soft) | 5 (Loose) |
| Dry densities ($\rho_d$ g/cm$^3$) | 0.5 | 0.6 | 1.4 |

## 4 PROTOTYPE MODEL TESTS

### 4.1 *Model ground types and measurements*

Prototype model tests were carried out at three types of model slopes (Cs1, Cs2 and Cs3). Cs1 was composed of Kanto loam without compaction, Cs2 was composed of Kanto loam with 5 cycles of roller compaction for each layer, and Cs3 was composed of Narita sand with 5 cycles of roller compaction for each layer.

The slopes were 45 degrees in inclination and 5m in height. 2.5m was provided as the width of each cut. Table 1 shows the conditions of the three types of model slopes. Figure 4 shows the distribution of interpreted N-values obtained from Swedish weight sounding tests during primary site studies. Of the three slopes, Cs1 had the lowest N-value.

The *SPS* was installed in a position 1m below the slope shoulder. A backhoe cut a distance of 0.5m from front to back during each step of the cutting process, as shown in Figure 5. An interval of 5 minutes was allowed between cuts, to observe possible slope movement.

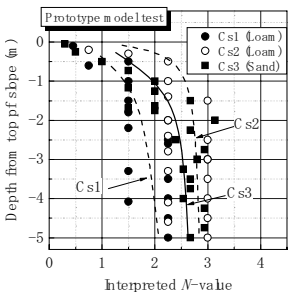


Figure 4. Distribution of interpreted N-values for model slopes

Figure 5. Overview of cuttings in prototype model test

### 4.2 *SPS reactions at Cs1*

Figure 6 shows the reaction of $r_s$ prior to failure at Cs1. Positive $r_s$ values correspond to the bending in convex upward. The ratio of the increment of the average angle of deflection in the *SPS* ($\Delta\theta_i$) to the increment of $r_s$ ($\Delta r_s$) is around 0.003 (%/$\mu\varepsilon$).

$r_s$ did not show any evident reaction at 11:20 a.m., just after completion of a series of cuttings. However, the slope failed at 11:32, a little more than ten minutes after cutting was completed. There was thus a time lag. Two bending points are seen in the $r_s$ curve. The first and second bending points are defined as BP1 and BP2, respectively. Values for the velocities of strain increments for both $V_1$ and $V_2$ are defined as the minimum absolute values of secant modulus for each bending point. The remaining times of both $t_{r1}$ and $t_{r2}$ indicate minutes up to the failure. $r_s$ shows a similar creep strain curve. BP1 was

recognized at 11:26, where $t_e$=63(min). A second creep was evident since $r_s$ decreased linearly by 2.7($\mu\varepsilon$/min) of $V_1$. Six minutes of $t_{r1}$ elapsed before the failure.

A third creep began at 11:30, where $t_e$=68(min). This was determined because the $r_s$ value accelerated after the evident bend. Two minutes of $t_{r2}$ remained at this BP2. The value of $V_2$ became much higher than that of $V_1$, and the slope failed catastrophically.

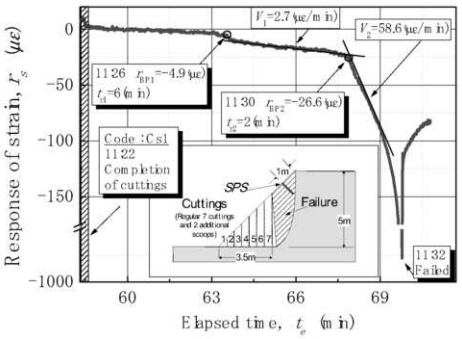


Figure 6. Response of strain ($r_s$) by *SPS* prior to failure at Cs1

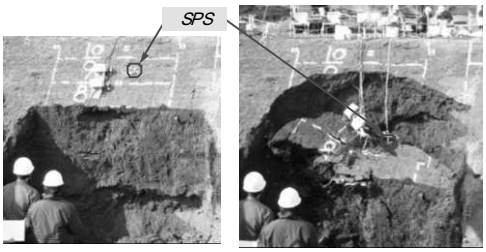


a) Two minutes before b) At beginning of failure

Figure 8. Observation of upcoming failure at Cs2

## 4.3 *SPS reactions at Cs2*

Figure 7 shows another relationship between $r_s$ and $t_e$ prior to failure at Cs2 (also Kanto loam). Figure 8 shows photos indicating the failure process. A slip surface developed beginning at a position 0.8m under the slope shoulder. However, no evident cracks or notable movement were observed two minutes before the failure.

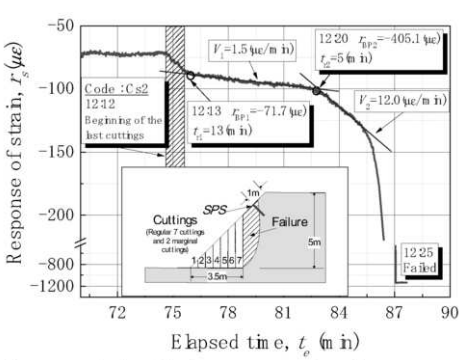


Figure7. Relationship between $r_s$ and $t_e$ prior to failure at Cs2

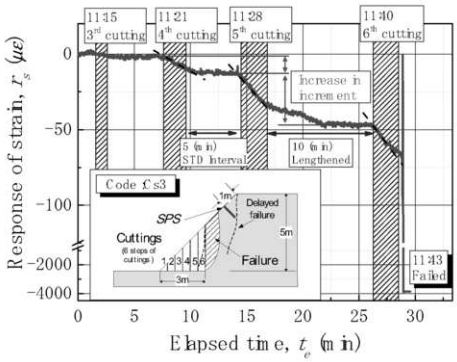


Figure 9. Relationship between $r_s$ and $t_e$ prior to failure at Cs3

BP1 appeared immediately after the last cutting at 12:13 p.m., where $t_e$=76(min). The beginning of the second creep was confirmed, with $r_s$ linearly decreasing by 1.2($\mu\varepsilon$/min) of $V_1$. The slope gradually became unstable, with the elapse of 13 minutes of $t_{r1}$. A third creep was observed beginning at 12:20, where $t_e$=82(min). The ratio of $V_2$ to $V_1$ reached approximately ten. The value of $r_s$ quickly decreased in a manner similar to pre-failure phenomena observed at Cs1. Then the slope failed catastrophically after 5 minutes of $t_{r2}$.

Curves at both Cs1 and Cs2 show a similar creep strain reaction. Determining the existence of either the second or third creep would provide workers with a couple of minutes' time for escape.

## 4.4 *SPS reactions at Cs3*

Figure 9 also shows the relationship between $r_s$ and $t_e$ prior to failure at Cs3. Recall that Cs3 was composed of compacted Narita sand. A small failure occurred early in the shallow section of the slope after the fourth cutting, because the self-supporting strength of the Narita sand was low due to a cohesive force less than that of Kanto loam. The value of $r_s$ decreased during the fourth cutting, but converged soon after completion of the cuttings.

Another failure followed in the upper shallow section after the fifth cutting, and the interval was lengthened to ten minutes for convergence in $r_s$. Since the failure surface mostly reached the position planned in the sixth cutting, soil deposited under the slope by the failure was only removed at this time. The slope failed largely after the sixth cutting. Increased shear strain in the shallow section, as measured by the *SPS*, corresponded to the slope becoming unstable. The value of $r_s$ decreased sharply, and the slope simply failed.

Consequently, $r_s$ did not show the creep strain tendency that was evident during two different phases of the second creep with linear decrease, or the third creep with accelerating decrease, as seen at both Cs1 and Cs2. $r_s$ at Cs3 repeatedly converged after the cuttings, while the reactions increased with the progress of the cuttings. However, an increase in shear strain in the shallow section of the slope, as measured by the *SPS*, mostly corresponds to an increase in the risk of failure. The reactions prior to failure are different, depending on the properties of the soil composing the slopes.

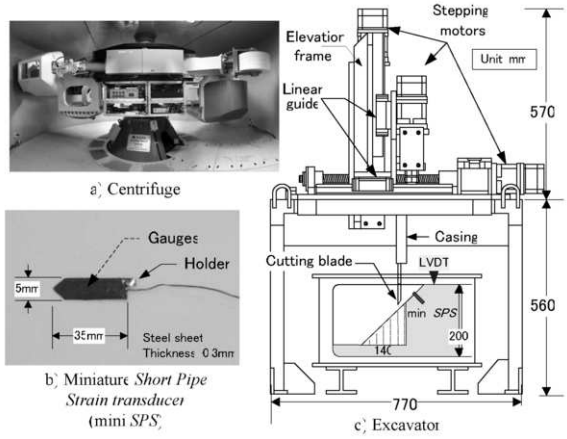


Figure 10. Apparatus and devices used in Centrifuge model tests

Table 2. Test conditions in centrifuge model tests

| Code | Cs4 | Cs5 |
|---|---|---|
| Soil material | Kanto loam | Narita sand |
| Corresponding prototype field tests | Cs1 | Cs3 |
| Centrifugal acceleration (g) | 30 | 25 |
| Numbers of cuttings | 7 | 8 |

## 5 CENTRIFUGE MODEL TESTS

Two sets of centrifuge model tests were carried out for additional *SPS* tests. Figure 10 shows an overview of the geotechnical centrifuge in NIOSH, Japan. Table 2 summarizes the testing conditions during the centrifuge model tests.

1/25 scale model slopes were prepared using the same soil materials and reproducing the same dry densities as those for the prototype model tests. An in-flight excavator (Tamrakar et al. 2006) was used to simulate the same cutting process as that used for the prototype model tests. Miniature short pipe strain transducers (mini *SPS*) were installed at the slope shoulders to measure the response of strain ($r_s$) as an increase of shear strain. The mini *SPS* were made of thin steel sheets that were 35mm in length, 5mm in width and 0.3mm in thickness. Linear variable differential transformers (LVDT) were set on the slope crowns to measure settlement ($s_t$).

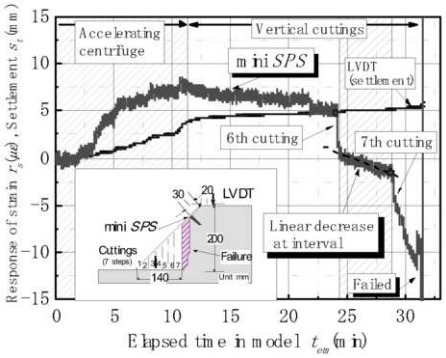


Figure 11. Time series reactions of $r_s$ and $s_t$ at Cs4

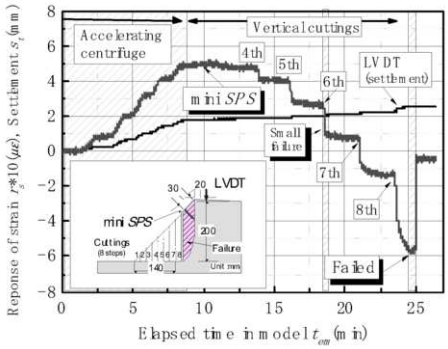


Figure 13. Time series reactions of $r_s$ and $s_t$ at Cs5

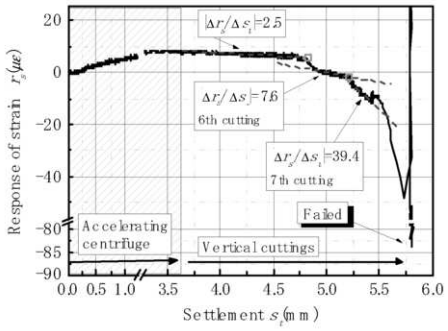


Figure 12. Relationship between $r_s$ and $s_t$ at Cs4.

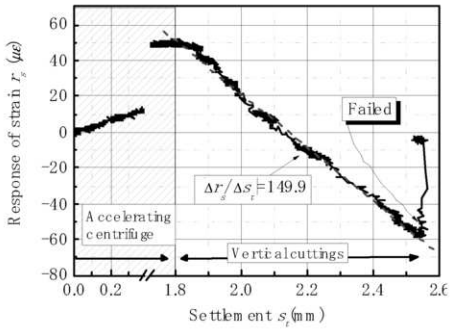


Figure 14. Relationship between $r_s$ and $s_t$ at Cs5.

## 5.1 *Reactions at Cs4*

Figure 11 shows the reactions of $r_s$ and $s_t$ at Cs4 (Kanto loam). Centrifugal acceleration increased from 0 to 30g when the elapsed time in model ($t_{em}$) was between 0 and 12. Seven steps of cuttings were carried out after 12(min) of $t_{em}$. The slope failed at 31(min) of $t_{em}$ soon after the seventh cutting. Curves of $s_t$ and $r_s$ both commonly react with cutting progression, although the increases were not as evident between the first and fifth cuttings. However, $r_s$ linearly decreased during the interval of $t_{em}$ between 24 and 29. This phenomenon was commonly seen at Cs1 and Cs2 during the prototype model tests.

Figure 12 indicates the relationship between $r_s$ and $s_t$. $|\Delta r_s/\Delta s_t|$ values show the absolute secant modulus of the curve at the three reference points. $r_s$ shows a tendency to decrease to $s_t$. $|\Delta r_s/\Delta s_t|$ values increase as the failure approaches. Consequently, increased shear strain in the shallow section indicated an increase in the risk of slope failure that was higher than that of settlement.

## 5.2 *Reactions at Cs5*

Figure 13 shows the reactions of $r_s$ and $s_t$ at Cs5 (Narita sand). Eight cutting steps were carried out at 25g. The slope failed soon after the eighth cutting, where $t_{em}$=25(min).

Both curves in $r_s$ and $s_t$ show a staged reaction in response to the cuttings. In addition, increments of the reactions increase as the cuttings progress. Moreover, the curve of $r_s$ shows the same staged increase as the curve at Cs3 (Narita sand) in the prototype model test.

Figure 14 shows the relationship between $r_s$ and $s_t$. Since $r_s$ decreases linearly to $s_t$, an increase in the shear strain in the shallow section is associated with settlement of the crown.

## 6 *SPS* APPLICABILITY

The experiments showed that shear strain in the shallow section of slopes increases in association with an increase in the risk of slope failure. They also confirmed that an increase in shear strain corresponds to settlement on the crown of slopes.

The installation of conventional sensors to measure settlement in the field involves difficulties. For example, a wire type of sensor requires both a fixed point and a moving point to measure ground displacement. However, *SPS* installation is easy because the screw point enables penetration into the shallow sections of slopes without pre-boring. The *SPS* would be effective in monitoring increased risk of slope failure in slopes that show a creep strain curve prior to failure.

## 7 CONCLUSIONS

Device applicability for monitoring increased shear strain in shallow sections of slopes was studied to determine any increase in the risk of slope failure. Several sets of prototype model tests and centrifuge model tests were carried out at model slopes composed of either Kanto loam or Narita sand. The increment of shear strain was measured by a developed short pipe strain transducer, the *SPS*.

Evident increases in the response of strain ($r_s$) were measured during slope cuttings in both types of tests. In slopes composed of loam, similar reactions to the creep strain curve were observed. A couple of minutes' time could be provided for escape by identifying either a second or third creep. In slopes composed of sand, a linear relationship was confirmed between $r_s$ and settlement at slope top. The $r_s$ reaction is in proportion to the instability of the slope.

Accordingly, an association between increased shear strain in the shallow section of slopes and increased risk of slope failure was confirmed. Monitoring the increase of shear strain in shallow sections can be effective for subsidiary warning systems that are intended to save workers' lives

## REFERENCES

Itoh, K., Toyosawa, Y., Tamrakar, S. B. & Horii, N. 2005. Analysis of labour accidents caused by slope failure. Landslide, *Journal of the Japan Landslide Society*, 41(6), 585-597.

Tamrakar, S.B., Toyosawa, Y., Itoh, K. & Timpong, S. 2006. Failure height comparison during excavation using in-flight excavator. *Proceedings of the International Conference on Physical Modelling in Geotechnics-6th ICPMG'06*, Vol.1, 385-390.

Tamate, S., Endo, A., Toyosawa, Y., Itoh, K. & Tamrakar, S.B. 2007. Experimental Analysis of Shallow Deformations in Slope Failure, *Conference Presentations of the 1st North American Landslide Conference*, 1016-1028.